Eur. Phys. J. B **37**, 301–309 (2004)
DOI: 10.1140/epjb/e2004-00060-x

THE EUROPEAN PHYSICAL JOURNAL B

Analysis of low temperature specific heat in the ferromagnetic state of the Ca-doped manganites

D. Varshney[a] and N. Kaurav

School of Physics, Vigyan Bhawan, Devi Ahilya University, Khandwa Road Campus, Indore 452017, India

Received 23 October 2003
Published online 2 April 2004 –

Abstract. The reported specific heat $C(T)$ data of the perovskite manganites $La_{1-x}Ca_xMnO_3$, with $x = 0.1$, 0.2 and 0.33, is theoretically investigated in the temperature domain $4 \leq T \leq 10$ K. Calculations of $C(T)$ have been made within the two component scheme: one is the Fermionic and the other is Bosonic (phonon or magnon) contribution. Lattice specific heat is well estimated from the Debye model and Debye temperature for Ca doped lanthanum manganites is obtained following an overlap repulsive potential. Fermionic component as the electronic specific heat coefficient is deduced using the band structure calculations for ferromagnetic metallic phase. Later on, for $x = 0.1$, following double exchange mechanism the role of magnons is assessed towards specific heat and find that at much low temperatures ($T < 10$ K), specific heat increases and show almost $T^{3/2}$ dependence on the temperature. We note that, the lattice specific heat is smaller for $x = 0.1$ when compared to that of magnon specific heat below 10 K. For $x = 0.2$, i.e., in the ferromagnetic metallic phase the magnon contribution is larger with the electron contribution while the reverse is true for $x = 0.33$. It is further noticed that in the ferromagnetic metallic phase, electronic specific heat is small in comparison to the lattice specific heat in low temperature domain. The present investigations allow us to believe that electron correlations are essential to enhanced density of state over simple Fermi liquid approximation in the metallic phase of $La_{1-x}Ca_xMnO_3$ ($x = 0.2$, 0.33). The present numerical analysis of specific heat shows similar results as those revealed from experiments.

PACS. 65.40.Ba Heat capacity – 72.80.Ga Transition-metal compounds – 74.25.Kc Phonons – 75.50.Cc Other ferromagnetic metals and alloys

1 Introduction

Doped manganese oxides $R_{1-x}A_xMnO_3$ (R^{3+} = La, Pr, Nd; A^{2+} = Ca, Sr, Ba) belong to a class of highly correlated electronic systems with a strong interplay between electronic and magnetic order and are widely focused from last one decade or so. One of the most eye-catching properties of the manganites is the influence of a magnetic transition on the electronic conduction. Jonker and Van Santen [1] discovered in 1950 that the resistance below the magnetic ordering, the Curie temperature (T_c), exhibits a positive thermal coefficient, indicating metallic-like behaviour and a negative gradient above T_c. This simultaneous occurrence of ferromagnetism and metallic conduction is qualitatively explained with Zener's idea of double exchange (DE), where the presence of the Mn^{3+}-Mn^{4+} mixed valence ions is responsible for both ferromagnetic coupling and charge transport [2]. Quite generally the antiferromagnetism in the doped manganites is associated with the superexchange coupling of the localized electron spins. Despite such remarkable DE interaction involving the transfer of the electron between neighboring Mn ions through the O^{2-}, it is stressed that an additional electron-phonon interaction must be invoked to reduce the electron kinetic energy at the metal-insulator (MI) transition [3] and have pronounced effect on transport properties.

We note that in the above-mentioned approaches [1–3], the importance of the Coulomb correlations have not been stressed, however these are believed to be one of the important key factors to control the transport properties in manganites [4]. Apart from this, the electron correlation in the degenerate orbitals has been pointed out long back by Goodenough [5] and Kanamori [6], it seem to be impossible to uncover the origin of the Colossal Magnetoresistance (CMR) effect without correct description of magnetic properties. All these phenomena are considered as relevant to unique electronic and magnetic structures of the perovskite-type manganites in which mutual coupling among the charge, spin, orbital and lattice degrees of freedom is of substantial importance and much attention has been paid in recent past.

Lattice and spin excitations have tremendous impact on transport properties in manganites. Dai et al. [7] have indicated the significant role of lattice excitations

[a] e-mail: vdinesh33@rediffmail.com

in the measurement of the neutron cross section for coherent elastic scattering. Kim and coworkers [8] have reported the phonon infrared (IR) spectra of polycrystalline $La_{0.7}Ca_{0.3}MnO_3$ sample and found shifts in frequencies of the transverse optic (TO) phonons across the MI transition for bending and stretching modes, which is comparable with predictions of DE interaction and lattice polaron model. This implies that the role of electron-phonon interactions is significant in the DE mechanism in the material under consideration.

Quite generally, the existence of strong electron correlations is believed to influence the magnetic ordering and the magnetic excitation spectrum. The spin dynamics can provide crucial information for determining the itineracy of the system, as well as the importance of the electron correlations. Oleś and Feiner [9] argued that the spin dynamics evolves with doping concentration x, in particularly the orbital fluctuations play a prominent role as the undoped antiferromagnetic insulating state is approached. In passing, we refer to the neutron scattering studies of the spin dynamics in the metallic ferromagnetic state of $La_{1-x}A_xMnO_3$ in the optimally doped regime with $x \sim 0.3$ for A = Pb [10]. The results essentially point to the standard spin dynamics of a conventional metallic ferromagnet. We may quote to the work of Lynn and coworkers [11] who have used inelastic neutron scattering to probe the spin wave dispersion for polycrystalline $La_{0.67}Ca_{0.33}MnO_3$ and document a spin stiffness that does not vanish at T_c ($D(0) = 170$ meV Å^2, $D(250) = 80$ meV Å^2). In addition, these researchers observe a central peak with a width broader than the spin wave peaks in intensity-energy scans at spin wave vector of about 0.07 Å. Other spin waves excitation studies in manganite perovskites have revealed similar feature [12,13].

Heat capacity measurements are understood to be an instructive probe in describing the low temperature properties of the materials. Among various manganites, hole doped $La_{1-x}Ca_xMnO_3$ system are widely analysed experimentally, due to different electronic and magnetic structure with carrier density. Ramirez et al. [14] have measured the specific heat in this system from room temperature down to 50 K. They subtract the lattice contribution and investigate charge and magnetic ordering behaviour for a wide range of doping concentrations with $x = 0.1$ to 0.9. It appears that in the absence of long-range ferromagnetic order, i.e., in para or antiferromagnetic phase below a characteristic temperature T_{CO}, where the charges freeze in a lattice of Mn^{3+} and Mn^{4+} ions, charge ordering (CO) state occurs. However, the metallic state can be obtained on melting the charge ordered state by application of external magnetic field. It is further emphasized that the simultaneous occurrence of electron and lattice ordering implies extremely strong electron-phonon coupling.

Later on, Smolyaninova et al. [15] have reported the low temperature specific heat of $Pr_{1-x}Ca_xMnO_3$ with and without external magnetic field. They found an anomalous excess specific heat C' of nonmagnetic origin in the CO state and it appears even in ferromagnetic metallic state, obtained on applied magnetic field, which implies coexistence of metallic and CO regions in the presence of induced magnetic field. In continuation, the specific heat of the doped manganites with divalent Ba and Sr substitution at the trivalent La site have also been reported, in the low temperature regime, for a particular doping concentration [16]. The concept of magnetic polaron has been introduced in the manganites to explain the transport and magnetic properties.

We may refer to the work of Okuda et al., who have investigated the critical behaviour of the metal-insulator transition by low-temperature resistivity and specific heat measurement of single crystals of $La_{1-x}Sr_xMnO_3$ [17]. The key points figured are: the change Debye temperature (θ_D) indicates an anomalous softening of the lattice or increase in cubic power of T in the specific heat occurs with the decrease of x ($0.1 \leq x \leq 0.3$). The reduction of specific heat on the application of magnetic field is attributed to the suppression of the thermal excitation of the spin wave. While to that, the reduction of Debye temperature (θ_D) with decreasing Sr content is ascribe as existing dynamic Jahn-Teller (or electron-lattice interaction) distortion.

Woodfield et al. [18] in the heat capacity measurements of $La_{1-x}Sr_xMnO_3$ (ranges from 0.1 to 0.3 and $T \leq 10$ K) manganites have noticed an upturn in specific heat, which points to the presence of Schottky type anomalies arising from the interaction of rare earth ions with crystalline field. Furthermore, experimentally it is well established that a T^2 characteristic of specific heat for $LaMnO_3$ which moves to disappear in the Sr-doped manganites. Also, hyperfine contribution in specific heat studies in manganite perovskites, subsisting by the large local magnetic field at the Mn nucleus due to electrons in unfilled shells has revealed similar features [19,20]. These studies demonstrate that the depending upon the doping concentration, electronic and magnetic structure, constrained the role of magnon contribution in specific heat. These heat capacity measurements [17–20] have motivated us to perform a systematic study on manganites.

Subsequently, Ghivelder et al. [21] have reported the heat capacity of $La_{1-x}Ca_xMn\ O_3$ for $x = 0.1$, 0.33 and 0.62 in the temperature range $4 \leq T \leq 10$ K and found that for samples having the ferromagnetic insulating or antiferromagnetic ordering exhibits spin wave signature in specific heat data. Salient features of the reported specific heat measurements includes a linear term (γT) at low temperatures for $x = 0.33$. The contribution to electronic term (γT) was extracted from the total heat capacity and is argued that this contribution is mainly due to the electronic heat capacity and emphasized that the specific heat can be resolved into a γT contribution with a finite value of γ and a lattice contribution. Hamilton and coworkers [22] have emphasized the absence of magnon contribution for ferromagnetic samples in metallic regime, as might be expected from the excitation of ferromagnetic spin waves. It is further stressed that the number of mass-enhancement mechanisms may be envisaged, like lattice polarons related to the dynamical JT

effect or Coulomb-interaction effects in connection with Sommerfield constant (γ).

On the theoretical side the explanation of specific heat behaviour for a wide doping concentration range has, therefore, been of considerable interest. The motivation is two fold: a) to reveal the importance of the Coulomb correlations which is significant in controlling the transport properties in manganites and b) to understand the role of magnons as well electron-phonon in specific heat of the ferromagnetic metal or insulator. It is indeed essential to find out if these novel materials get their metal to insulator transition from an extremely strong interaction within the double-exchange mechanism and electron-lattice interaction or if any entirely new excitation has to be invoked. The specific heat measurement in $La_{1-x}Ca_xMnO_3$ has been thoroughly investigated for the ceramics sample so far, and we believe that the importance of the nearest-neighbour interactions as well as correlation among the charge carriers to explain the low temperature specific heat needs detailed investigations.

No systematic theoretical efforts addressing the issues of Coulomb correlations, spinwave impact and lattice contribution as well the competition among these process have been made so far, and in the present investigation, we attempt to understand them and retrace the reported specific heat behaviour. We begin with the assumptions and motivate them by simple physical arguments before taking up the details of numerical results obtained. The idea we have in mind is to focus attention on the subsisting mass-enhancement mechanisms in the ferromagnetic metallic regime. We employ the density of states as deduced from electronic energy band structure calculations and free electron approach in order to estimate the electronic specific heat for metallic region. In the case of manganites, separation of spin wave contribution from the lattice effect is difficult without an accurately estimation of Debye temperature. Also, it is worth to seek the possible role of phonons and magnons in the low temperature specific heat of manganites that has immediate important meanings to reveal the phenomenon of colossal magnetoresistance.

The present investigations are structured as follows. In Section 2, we introduce the model and sketch the formalism applied. As a first step, we estimate the Debye temperature following the inverse-power overlap repulsion for nearest-neighbour interactions in an ionic solid. We follow the Debye method to estimate the specific heat contributions of phonons and magnons. Developing this scheme for phonons, electrons and magnons specific heat, we have computed the low temperature specific heat of $La_{1-x}Ca_xMnO_3$ manganites for doping concentration $x = 0.1$, 0.2 and 0.33. In Section 3, we return to a discussion of results obtained by way of heat capacity curves. The final part of the paper is devoted to conclusions obtained and is summarised in Section 4. The purpose of what follows is to improve our understanding of Coulomb correlations, spinwave impact and lattice contribution in Ca doped manganites. We believed that detailed information on physical parameters in correlated electron system, as manganites can be understood by low temperature specific heat behaviour.

2 The model

We start by giving a brief description of the $La_{1-x}Ca_xMnO_3$ manganites. $LaMnO_3$ is best characterized and the most studied of the manganites. In the DE framework, the overlapping of the manganese and oxygen orbitals depends on the geometric arrangement of the ions. The bandwidth of the conduction band is primarily determined by the overlapping of the manganese and oxygen. The larger the overlap, the wider the band. For a given distance between the manganese and oxygen ions the overlap is largest when the Mn-O-Mn bond angle is 180°. Such structure, in which a manganese and six oxygen ions form regular octahedra (as shown in Fig. 1). But if lanthanum is replaced with a smaller ion, the octahedra buckle and the bond angle becomes smaller. The DE interaction consists of the transfer of the electron between neighbouring Mn ions through the O^{2-}. The Mn^{4+} ions have three d electrons, with t_{2g} symmetry, which are localized at the Mn sites. Along with these t_{2g} electrons, the Mn^{3+} ions have a fourth electron, an e_g electron, which is not localized and can be transferred between adjacent Mn ions through the path Mn-O-Mn. Because of the strong onsite Hund's coupling, at a Mn site the t_{2g} and e_g electrons have parallel spins. When the e_g electrons moves from one Mn site to another Mn site, it preserves its spin direction and couples with the corresponding t_{2g} electrons, leads to an effective ferromagnetic interaction between neighbouring Mn spins. Henceforth, bond distances play a crucial role in governing the properties of manganites. We begin with the lattice contribution towards specific heat.

2.1 Lattice specific heat

The acoustic mode frequency, shall be estimated in an ionic model using a value of effective ion charge $Ze = -2e$. The Coulomb interactions among the adjacent ions in an ionic crystal in terms of inverse-power overlap repulsion as [23]

$$\Phi(r) = -(Ze)^2 \left[\frac{1}{r} - \frac{f}{r^s}\right], \tag{1}$$

f being the repulsion force parameter between the ion cores. The elastic force constant κ is conveniently derived from $\Phi(r)$ at the equilibrium inter-ionic distance r_0 following

$$\kappa = \left(\frac{\partial^2 \Phi}{\partial r^2}\right)_{r_0} = (Ze)^2 \left[\frac{s-1}{r_0^3}\right]. \tag{2}$$

Here, s is the index number of the overlap repulsive potential. Then we use, acoustic mass $M' = (2M_+ + M_-)$ [Mn (O) is symbolised by $M_+(M_-)$], $\kappa^* = 2\kappa$ for each

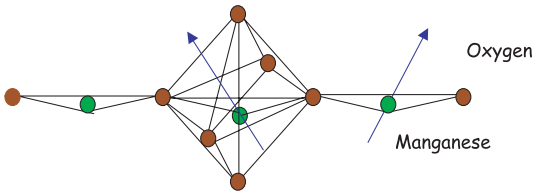

Fig. 1. Schematic diagram showing the regular octahedra.

directional oscillation mode to get the acoustic phonon frequency as

$$\omega_D = \sqrt{\frac{2\kappa^*}{M'}}, \\ = 2(Ze)\sqrt{\frac{(s-1)}{M'}\frac{1}{r_0^3}}. \quad (3)$$

Quite generally, the specific heat is dominated by quantized lattice vibrations (phonons) and is well estimated by conventional Debye theory. As phonons are bosons and waves of all frequencies in the range $0 < \omega < \omega_m$ (where ω_m is the maximum phonon frequency) could propagate through crystal. The internal energy of the crystal when the maximum energy of the phonons in the crystal $x = h\omega/k_BT$, is [24]

$$U = U_0 + 9Nk_BT\left(\frac{T}{\theta_D}\right)^3 \int_0^{\theta_D/T} \frac{x^3}{(e^x-1)}dx. \quad (4)$$

The specific heat from lattice contribution is obtained by temperature derivative as

$$C_{Ph} = 9Nk_B\left(\frac{T}{\theta_D}\right)^3 \int_0^{\theta_D/T} \frac{x^4e^x}{(e^x-1)^2}dx. \quad (5)$$

with θ_D as the Debye temperature and N is the number of atoms in a unit cell. We shall now switch to the estimation of electronic contribution.

2.2 Electronic specific heat

The temperature derivative of the internal energy yields the specific heat and is [24]

$$C_{el} = \frac{\pi^2}{3}k_B^2N\left(E_F\right)T = \gamma T \quad (6)$$

where $N(E_F)$ is the density of state at Fermi level and γ denotes the Sommerfield constant. It is evident from equation (6) that the electronic specific heat is influenced by the effective mass of the carriers as well by the carrier concentration, which are associated with density of states. Electron correlation effects are well known to be important for the transition-metal oxides and the importance of renormalization in mass due to electron-phonon interaction [25] and electron correlations for the perovskites is assessed in the later section.

2.3 Spin wave specific heat

Magnons obey Bose statistics and allow us for the calculation of the low-temperature thermal properties of magnetic materials. Only long-wavelength spin waves are excited at low temperatures and the dispersion relation for magnons in a spin system:

$$\omega(k) = \Delta + D_{stiff}k^2. \quad (7)$$

Here, the spin wave excitation at zero field is assumed and D_{stiff} (or D) is the spin-stiffness, which is a linear combination of the exchange integrals. Δ being the anisotropy spin wave gap.

The internal energy of unit volume due to magnon spin wave in thermal equilibrium at temperature T is given by [26]

$$U_{mag} = \frac{k_BT}{4\pi^2}\left(\frac{k_BT}{D_{stiff}}\right)^{3/2} \int_0^{x_m} \frac{x^{3/2}}{(e^x-1)}dx, \quad (8)$$

where $x = [\Delta + D_{stiff}k^2]/k_BT$. The specific heat is usually obtained by temperature derivative for long-wavelength spin waves, which are the dominant excitations at low temperatures, as

$$C_{mag} = \frac{k_B}{4\pi^2}\left(\frac{k_BT}{D_{stiff}}\right)^{3/2} \int_{\Delta/k_BT}^{\infty} \frac{x^{5/2}e^x}{(e^x-1)^2}dx. \quad (9)$$

Henceforth, the total contribution to specific heat is

$$C_{tot} = C_{ph} + C_{el} + C_{mag} \quad (10)$$

where, first term on the right side C_{ph} is the phonon contribution and varies as βT^3 [$T \ll \theta_D/10$], the coefficient β is related to the Debye Temperature θ_D. Second term C_{el} is the fermionic contribution γT, the linear coefficient (γ) can be related to the density of states at the Fermi surface. Last term, C_{mag} is associated with ferromagnetic spin wave excitations and vary as $\delta T^{3/2}$ in the low temperature regime ($\leq$10 K). Terms with higher powers of T than T^3 are anharmonic corrections to the lattice contribution and are ignored for the sake of simplicity in the present studies.

Having discussed the heat capacity contributions by phonons, electrons and magnons, we shall now estimate and compute numerically the specific heat of $La_{1-x}Ca_xMnO_3$ manganites. Obtained results along with discussion are presented in the following section.

3 Discussion and analysis of results

Any discussion of the manganites necessitates knowledge of the crystal structure, and this is particularly true of the calculations reviewed here. Special attention is paid in this approach to address the concept of electron correlations and mass renormalization effects on the heat capacity behavior. We begin with the discussion of phonon

behaviour of specific heat. There can be orthorhombic, rhombohedral and cubic phases in entire range of doping both as a function of temperature and as a function of concentration. While calculating the Debye temperature, we take $s = 9-11$ and the in-plane Mn-O distance $r_0 = 1.954$ {1.94, 1.96} Å [27] {[27], [28]}, for $x = 0.1$ {0.2, 0.33}, yielding $\kappa = 13.4$ {15.1, 15.2} $\times 10^4$ gms^{-2} due to the fact that the chemical pressure induces different bond length with composition. It is useful to point out that for correlated electron systems as cuprates, the index number of the repulsive potential has been reported to be $s = 10$ [29]. With these parameters, the Debye frequency is estimated as 33.4 meV (387 K), 35.3 meV (410 K) and 35.5 meV (412 K), and is essential for estimation of the phonon contribution in specific heat for the samples $x = 0.1$, 0.2 and 0.33, respectively.

The Debye temperature (θ_D) 387 K, 410 K and 412 K, yields $\beta = 0.168$, 0.141 and 0.139 mJK^{-4} mol^{-1} for $x = 0.1$, $x = 0.2$ and 0.33, respectively. It is noticed that θ_D increases substantially from the paramagnetic insulator (0.1) to ferromagnetic metallic phase (0.33). The calculated values of the Debye temperature and lattice term are consistent with the specific heat measurements ($\theta_D = 368$ K for $x = 0.1$) of $La_{1-x}Ca_xMnO_3$ manganite [21]. However, we do not claim the process to be rigorous, but a consistent agreement following overlap repulsion is obtained on Debye temperature as those revealed from specific heat data. Usually, the Debye temperature is a function of temperature and varies from technique to technique. Values of the Debye temperature also vary from sample to sample with an average value and standard deviation of $\theta_D = \theta_D \pm 15$ K. With the above-deduced values of θ_D, the change in θ_D with x indicates that a reduction of T^3-term in the specific heat occurs with the elevated values of x (0.1 to 0.33). To explain the variation of θ_D with the Ca substitution, we attempt to analyze our results in the framework of DE interaction with electron-lattice interaction. The change of the Mn-O distance induced by substitution of the La site by Ca increases θ_D. Henceforth, the x dependence of θ_D in $La_{1-x}Ca_xMnO_3$ suggests that increased hole doping drives the system effectively toward the weak electron-phonon coupling region.

So far, we have only discussed the phonon and electron contribution to heat capacity. Yet the heat capacity measurements shall be used to probe the magnetic excitations in magnetic systems and we complete our numerical analysis by understanding the magnon contribution to the specific heat. For $x = 0.1$, the material is ferromagnetic at low temperatures and displays insulating behavior at all temperatures [30]. The spin wave stiffness coefficient is evaluated following $D = 2JSa^2$, where S (average value of the spin) and J (magnetic exchange coupling parameter) are directly related as $S = (4 - x)/2$ and $J = T_c k_B/4S(S + 1)$ [10], to get $D = 39.3$ meV Å^2 and the magnon contribution $\delta = 5.6$ mJ K$^{-5/2}$ mol^{-1} for $x = 0.1$. Here, the lattice parameter a is 3.87 Å and T_c being the Curie temperature and is about 180 K. With the above-deduced model parameters, the specific heat due to both magnons and phonons is plotted with temperature for $x = 0.1$ in Figure 2. At much low temperatures ($T < 10$ K), specific heat increases and show almost $T^{3/2}$ dependence on the temperature and is attributed to the magnon participation for specific heat.

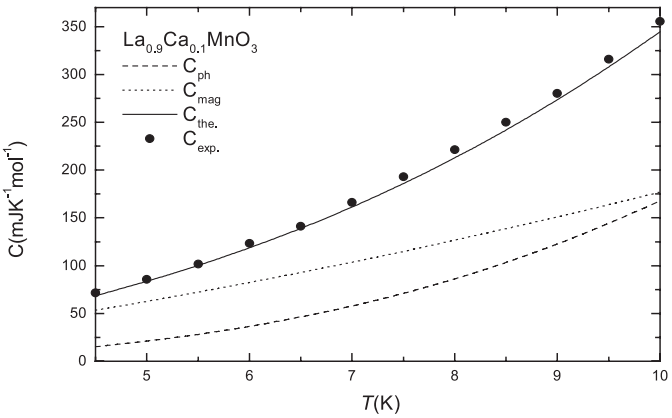

Fig. 2. Variation of specific heat with temperature. Solid circles are experimental data taken from Ghivelder et al. 1998.

Furthermore, the lattice specific heat follows a conventional T^3 characteristic and is noticed from the curve that the specific heat from lattice contribution is less to that of magnon specific heat in the temperature domain under consideration. Both the contributions are clubbed and the resultant is plotted along with the experimental [21] data in same figure. We find similar results of heat capacity as those revealed from experiments. The consistency is attributed to the proper estimation of Debye temperature from an inverse power overlap repulsion as well other free parameters (spin wave stiffness, average value of the spin and magnetic exchange coupling parameter). It is worth to point out that δ remains unchanged for low temperatures ($\leq$10 K), while to that it varies exponentially with temperature for $T \geq 10$ K as evident from equation (10). Henceforth, a T^3 contribution from the lattice and a $T^{3/2}$ contribution from the spin wave motion yield the consistent interpretation of specific heat in the present calculations for ferromagnetic insulator. We may record the fact that Ghivelder et al. [21] obtained a better agreement of the theoretically estimated lattice and magnon specific heat with that of reported data. The consistency arose from the fact that the authors have estimated θ_D from the heat capacity data, while to that in the present model calculations, θ_D is obtained for an overlap repulsive potential.

To gain an additional insight in to the observed metallic behaviour in the low temperature domain, it is worth to address the possible role of mass renormalization of carriers due to differed values of γ obtained from electron energy band structure calculation and specific heat measurements. For $x = 0.33$, the manganite has ferromagnetic ordering and shows the signature of magnons in inelastic neutron scattering data [11]. Perhaps the dilemma in determining the magnetic specific heat of manganites is that it represents the spin-wave stiffness and anisotropy related with spin-wave gap. The stiffness is proportional to T_c and S, where T_c is the Curie temperate and S being

the average value of the spin, whereas, anisotropy gap has been determined from neutron-scattering results and is about 0.04 meV for $La_{0.67}Ca_{0.33}MnO_3$ [11]. A small value of gap in these materials would be sufficient to add a FM spin wave contribution. Henceforth, the specific heat due to magnons is also of importance in the metallic state of $La_{1-x}Ca_xMnO_3$.

We deduce the stiffness coefficient D as 115 meV Å^2 and the spin wave contribution δ of about 1.15 mJ K$^{-5/2}$ mol^{-1} for $x = 0.2$. In the following calculations, we have used $a = 3.9$ Å and T_c of about 250. Furthermore, we use $D = 170$ meV Å^2 from inelastic neutron scattering [11] to get $\delta = 0.62$ mJ K$^{-5/2}$ mol^{-1} for $x = 0.33$. By above intrinsic fashion followed by these composition the experimental data can be fitted qualitatively by Debye temperature of 410 K and 412 K, which yields $\beta = 0.141$ mJ K^{-4} mol^{-1} and $\beta = 0.139$ mJ K^{-4} mol^{-1} for $x = 0.2$ and 0.33, respectively. It is worth to point out that the θ_D[=391 (430) K] is obtained at $x = 0.2$ (0.33) [22]([21]). In the present calculations, index number of the repulsive potential is a free parameter and we obtained a larger value of θ_D as compared to reported data in the ferromagnetic metallic phase.

We shall now address the importance of the Coulomb correlations, which is of importance in revealing the transport properties in manganites. Using density of state at the Fermi surface $N(E_F) = 5 \times 10^{23}$ eV^{-1} mol^{-1} from the electron energy band structure calculations [31] at $x = 0.33$ for both a ferromagnetic cubic perovskite and a ferromagnetic *Pnma* structure, we find $\gamma = 1.96$ mJ K^{-2} mol^{-1}. On the other hand, enhanced $\gamma_{exp.}$ (=4.7 mJ K^{-2} mol^{-1}) is extracted from the low temperature specific heat data [21]. It is instructive to mention that the band structure studies does not incorporate the Coulomb correlations and electron phonon interaction. Difference in γ_b and γ_{exp} necessarily points to the importance of mass renormalization of carriers and indeed significant in manganites. Infact, the effective charge carrier mass is sensitive to the nature of interaction in Fermi liquid description. However, in the CMR materials the electron-electron interactions are apparently important as e_g electrons also interact with each other via the Coulomb repulsion. Precisely, the enhancement of the γ due to electron correlations in manganites is, therefore, necessarily to be incorporated.

The importance of renormalization in mass due to electron correlations and electron-phonon interaction for the perovskites is evaluated following

$$\frac{\gamma_{\text{exp.}}}{\gamma_b} = \frac{m^*}{m_e}. \tag{11}$$

On the other hand, if we incorporate the electron-phonon coupling, the electronic specific heat coefficient will take the following form:

$$\gamma = \frac{\pi^2}{3} k_B^2 N(E_F)(1+\lambda). \tag{12}$$

λ being the electron-phonon coupling strength and is characteristic of a Jahn-Teller material. Naturally, the electronic specific heat constant is directly proportional to the density of states of the electron at the Fermi level. It is worth to stress that the understanding of the electronic specific heat coefficient (γ) is quite relevant as it is a direct measurement of fundamental property of metallic materials. While estimating effective mass, following equation (11), we find $\gamma = 2.4\gamma_b$ and is either due to Coulomb correlations or electron-phonon/magnon interaction for $x = 0.33$. Similar enhancement in γ is reported earlier and is mainly from correlation effects in the $La_{1-x}Sr_xTiO_3$ system, undergo to metallic by Sr doping [32].

The Coulomb correlations effect for mass renormalization is important in metal oxides. We may refer to an earlier work of Synder et al. [33], who have reported the quadratic temperature dependent resistivity of $La_{0.67}Ca_{0.33}(Sr_{0.33})MnO_3$, which points to electron-electron interaction. Furthermore, the non-linearity in the temperature-dependent resistivity behaviour is attributed to electron-electron scattering. The resistivity behaviour follows power temperature dependence over a low temperature domain and a better argument is observed using a T^2 term, which, it is argued, is evidence of electron-electron scattering. Accordingly, electron-electron scattering has been predicted from a magnetic material with a low-carrier density (5.65×10^{21} cm^{-3}) for the $La_{0.67}Ca_{033}MnO_3$ system. The carrier density is comparable to those for other perovskite oxide [16]. It worth to point out that, using the Fermi-liquid relation: $N(E_F) = 3n/2E_F$, we find an upper bound on the Fermi energy of about 0.6 eV. In principle the electron-electron scattering is proportional to $(1/E_F)^2$ and hence small Fermi energy enhances the electron-electron scattering [34].

Apart from Coulomb correlations, mass renormalization is also made possible due to electron-phonon interaction in manganites. Indeed, the charge carriers interact with each other and with distortions of the surrounding lattice, i.e., with phonons. We believe that the electron-phonon strength, λ, is not involved in mass renormalization of carrier in order to enhanced γ for such a low temperature domain. The idea we have in mind is that the electron-phonon coupling localizes the conduction band electrons, as polarons become stronger well above to the transition temperature. Furthermore, nature of polaron changes across T_c and a crossover from a polaronic regime to a Fermi liquid like regime, in which the electron-phonon interaction is insufficient to localize the electrons when T tends to zero [3]. This result suggests that the mass renormalization due to electron-phonon interactions is not of overwhelming importance in the metallic state of $La_{1-x}Ca_xMnO_3$ ($x = 0.2$ and 0.33). It is thus inferred that the Coulomb correlations have a pronounced effect, which was not considered in the band structure calculation to deduce the electronic specific heat coefficient γ in the metallic state.

Besides, the Coulomb correlations and the electron-phonon interaction, another possibility for the carrier mass renormalization arose due to the presence of spin waves in the metallic system, and is caused by spin wave scattering at low temperature. It is worth referring to an

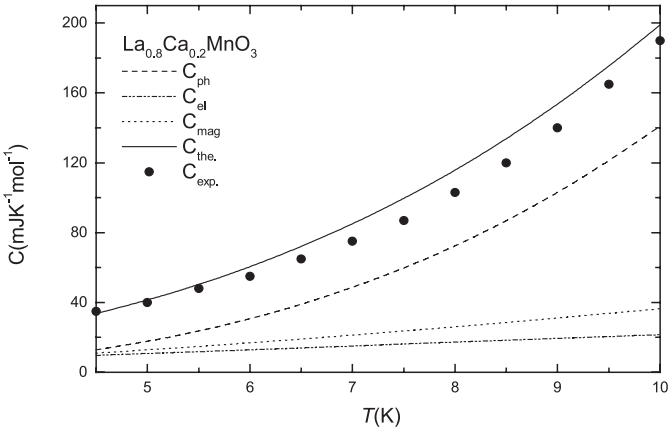

Fig. 3. Variation of specific heat with temperature. Solid circles are experimental data taken Hamilton et al. (1996).

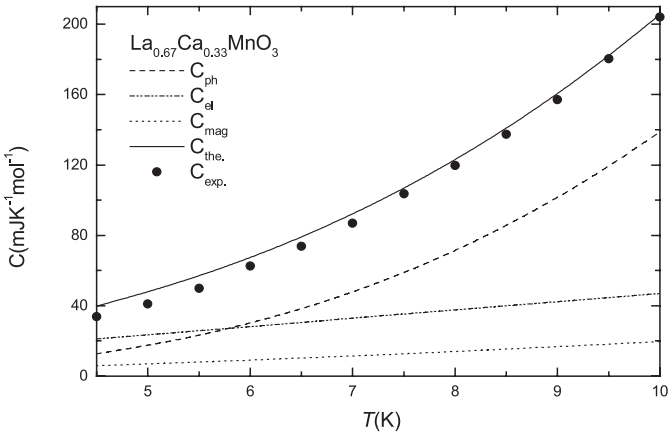

Fig. 4. Variation of specific heat with temperature Solid circles are experimental data taken from Ghivelder et al. (1998).

earlier work of Fulde and Jensen [35], who have argued that electron mass is also enhanced by interaction with spin wave in manganites. From the band structure calculations, it is widely believed that at low temperatures $La_{0.67}Ca_{0.33}MnO_3$ is half-metallic [31]. This necessarily points to the fact that the conduction is limited to a single Mn spin up channel of majority carriers. However, the Mn spin down channels are localized, henceforth, the normal emission and absorption of spin waves at finite temperatures are forbidden. As a result there are no conducting state at low energy to scatter into spin flip. It is worth to stress that the low-temperature spin wave scattering for the up-spin channel is mainly due to phonons, or to spin conserving electron-electron processes.

Due to unavailability of band structure data for $N(E_F)$ at $x = 0.2$, we have employed the free electron estimation with similar enhancement in order to calculate the electronic specific heat coefficient γ (=2.16 mJ K^{-2} mol^{-1}). However, we can not use available $N(E_F)$ for $x = 0.33$ because of the fact that the T_c is different and in the double exchange (DE) model, T_c is proportional to the effective transfer integral t for electrons hopping between Mn ions. Furthermore, the density of states at the Fermi energy, $N(E_F)$, is inversely proportional to t within the tight binding approximation.

Figures 3 and 4, show the results of temperature dependence of specific heat for $x = 0.2$ and 0.33. The contributions of phonon, electron and magnon to specific heat are shown separately along with the total specific heat. It is inferred from the plots that, in the low temperature domain phonons play significant role, electronic specific heat varies linearly with temperature and less to phononic component. It is noteworthy to comment that, in manganites, the electron contribution to the specific heat can at best be seen only at very low temperature due to its small magnitude when a comparison is made with phonon contribution. It is further noticed from Figures 3 and 4 that in the ferromagnetic metallic state i.e., for $x = 0.2$, the magnon contribution is larger with the electron contribution while the reverse is true for $x = 0.33$.

The observed increase of γ with x from $x = 0.1$ to $x = 0.33$ demonstrates strong electron correlations in manganites and is in accord with tendency that the large Coulomb interaction U suppresses the double occupancies of e_g electrons. Furthermore, x-induced reduction of magnon specific heat can therefore be explained in terms of Ca doping dependence of magnon stiffness constant (D). The change in D indicates that a softening of the spin or decrease of $T^{3/2}$-term in the specific heat occurs with the increase of x ($0.1 \leq 0.33$). It is worth to argue that one of the possible accounts for this x-dependent change of D is to assign this to the existence of Coulomb correlations down to low or zero temperature. In fact, the strong correlations in an over doped region points to metallic characteristic. However, in the region of $x = 0.1$–0.33 the correlation effects among the carriers is enhanced by hole motion as gradual release of kinetic energy when the hole concentration increases and accordingly the magnon contribution may be much reduced as observed. The present numerical calculations strongly support the idea of Oleś and Feiner [9] who argue that the spin wave stiffness coefficient is isotropic and increases with hole doping in the ferromagnetic metallic phase of manganites following t-j model. They emphasized that the gradual release of the kinetic energy in a correlated system when the carrier concentration increases and noticed that this is possible only when the local correlations between e_g electrons are invoked.

4 Conclusion

The heat capacity, i.e., specific heat (C) behaviour is believed to be an instructive probe of understanding the role of phonons, electronic and spin wave excitations in manganites. In order to simulate the actual situation occurring in the temperature dependent behaviour of specific heat in manganites, we have outlined the theory and analysed the available experimental data by assuming three channels to heat capacity: phonon, electron and magnon.

We follow Debye model within harmonic approximation in low temperature regime and used Debye temperature following the inverse-power overlap repulsion for nearest-neighbour interaction. While computing specific heat we use spin wave stiffness, average value of the spin and magnetic exchange coupling as free parameters. Developing this scheme, the present investigation deals with a quantitative description of temperature dependent behaviour of specific heat in manganites. In the present study, we employ more realistic values of physical parameters determined from the available experimental and theoretical data.

The proposed analysis reveals an independent estimation of lattice specific heat within the harmonic approximation by proper utilisation of the Mn-O distance. With the above-deduced values of θ_D, the change in θ_D with x indicates that a reduction of the lattice stiffness or increase of T^3-term in the specific heat occurs with the decrease of x ($0.1 \leq x \leq 0.33$). To explain the variation of θ_D with the Ca substitution we attempt to analyse our results in the framework of DE interaction with electron-lattice interaction. Partial substitution of Ca at the La site in the parent compound changes the bond length and hence leads in an increase in θ_D. Thus, the Ca doping dependence of θ_D suggests that hole doping drives the system effectively toward the weak electron-phonon coupling strength. Values of θ_D from the present calculation are comparable as those revealed from heat capacity data. For $x = 0.1$, specific heat increases and show almost $T^{3/2}$ dependence on the temperature and are attributed to spin wave contribution. We found that a simple analysis head of the specific heat into a T^3 contribution from the lattice and a $T^{3/2}$ contribution from the spin wave excitation yields the correct interpretation of ferromagnetic insulator. Although the contribution of spin wave excitations at the doping concentration $x = 0.1$ is larger in comparison to lattice specific heat, a consistent explanation of the experimental data demands the presence of both components.

The appropriateness of the present analysis depends on the understanding of band-structure estimation of density of state. Fermionic component as the electronic specific heat coefficient is deduced following the density of state from electronic energy band-structure calculation and free electron estimations. We have incorporated the Coulomb correlations and electron-phonon coupling strength while estimating the electronic specific heat coefficient γ and we believe that both of these have important implication in describing the electronic channel to the heat capacity in doped manganites. The electron scattering rate at low temperature is inversely proportional to Fermi energy ($E_F \approx 0.6$ eV) and value of E_F is low in doped manganites as compared to conventional metals, which implies that Coulomb correlations may dominate over other excitations (lattice and spin wave) in the low temperature domain ($T \leq 10$ K). In passing, we appeal that mass enhancement in the electronic channel may consistently retrace the experimental results for the specific heat at low temperature (mass of carriers is enhanced by a factor of 2.4 to that of bare mass of electron). It is inferred from the above analysis that, in the low temperature domain, electronic specific heat varies linearly with temperature and phononic term has pronounced effects in the ferromagnetic metallic phase. Furthermore, the magnon specific heat in the ferromagnetic metallic state of Ca doped manganites have relevance due to negligible anisotropy gap as revealed from neutron scattering data. It is noticed that for $x = 0.2$, i.e., in the ferromagnetic metallic phase the magnon contribution is larger with the electron contribution while the reverse is true for $x = 0.33$. These findings express that the large Coulomb interaction U suppresses the double occupancies of e_g electrons and enhanced electronic specific heat, while the decrease of $T^{3/2}$-term with Ca doping concentration.

To an end, the retraces of the heat capacity experimental curve in La-Ca-MnO_3 is attributed to the assumption that the phonons in the temperature domain $5 \leq T \leq 10$ K are thermally mobile in the ferromagnetic metallic phase of manganites and are usually the major component of specific heat. As θ_D is about 350–450 K in manganites, the Debye model with $T \ll \theta_D/10$ is meaningful at low temperatures. The fermionic contribution to the specific heat can at best be seen only at very low temperature due to its small magnitude when a comparison is made with phonon contribution. The electronic specific heat allows us to analyse the metallic behaviour in the composition ranging from 0.2 to 0.33 and mass enhancement due to Coulomb correlations have significant implications. We note that the present model calculation also points to the importance of spin wave excitations explicitly in the ferromagnetic insulator phase where the spin wave component is dominating over the lattice specific heat. In continuation, the spin wave excitations are also important in the ferromagnetic metallic phase in view of inelastic neutron scattering results. We believe that the proper incorporation of the realistic physical parameters based on experimental observation will lead to a clear picture of the low temperature transport properties in manganites.

Conclusively, we have made an attempt to analyse the reported heat capacity behavior in doped manganites based on three component model. The scheme opted in the present study is so natural that it extracts only the essential contributions to describe the heat capacity behavior. We should emphasize that in order to carry out a complete and consistent comparison between theory and experiment, it is therefore necessary to include the effects brought about by electron correlations and mass renormalizations by electron-phonon interaction and spin wave effects in magnetic systems as doped manganites. Although we have provided a simple explanation of these effects, there is a clear need for good theoretical understanding of the heat capacity behavior in manganites.

Financial assistance from Madhya Pradesh Council of Science and Technology, Bhopal is gratefully acknowledged.

References

1. G.H. Jonker, J.H. Van Santen, Physica **16**, 337 (1950); J.H. Van Santen, G.H. Jonker, Physica **16**, 599 (1950)
2. C. Zener, Phys. Rev. **82**, 403 (1951); P.W. Anderson, H. Hasegawa, Phys. Rev. **100,** 675 (1955)
3. A.J. Millis, P.B. Littlewood, B.I. Shrainman, Phys. Rev. Lett. **74**, 5144 (1995); A.J. Millis, B.I. Shrainman, R. Mueller, Phys. Rev. Lett. **75**, 175 (1996)
4. T. Mizokawa, A. Fujimori, Phys. Rev. B **51**, 12880 (1995)
5. J.B. Goodenough, Phys. Rev. **100**, 564 (1955)
6. J. Kanamori, J. Phys. Chem. Solids **10**, 87 (1959)
7. P. Dai, J. Zhang, H.A. Mook, S.-H. Liou, P.A. Dowben, E.W. Plummer, Phys. Rev. B **54**, R3694 (1996)
8. K.H. Kim, J.Y. Gu, H.S. Choi, G.W. Park, T.W. Noh, Phys. Rev. Lett. **77**, 1877 (1996)
9. A.M. Oleś, Louis F. Feiner, Phys. Rev. B **65**, 052414 (2002)
10. T.G. Perring, G. Aeppli, S.M. Hayden, S.A. Carter, J.P. Remeika, S.-W. Cheong, Phys. Rev. Lett. **77**, 711 (1996)
11. J.W. Lynn, R.W. Erwin, J.A. Borchers, Q. Huang, A. Santoro, Phys. Rev. Lett. **76**, 4046 (1996)
12. M.C. Martin, G. Shirane, Y. Endoh, K. Hirota, Y. Moritomo, Y. Tokura, Phys. Rev. B **53**, 14285 (1996)
13. F. Moussa, M. Hennion, J. Roderiguez-Carvajal, H. Moudden, L. Pinsard, A. Revcnolevschi, Phys. Rev. B **54**, 15149 (1996)
14. A.P. Ramirez, P. Schiffer, S.-W. Cheong, C.H. Chen, W. Bao, T.T.M. Palstra, P.L. Gammel, D.J. Bisho, B. Zegarski, Phys. Rev. Lett. **76**, 3188 (1996)
15. V.N. Smolyaninova, A. Biswas, X. Zhang, K.H. Kim, Bog-Gi Kim, S.-W. Cheong, R.L. Greene, Phys. Rev. B **62**, R6093 (2000)
16. J.M.D. Coey, M. Viret, L. Ranno, K. Ounadjela, Phys. Rev. Lett. **75**, 3910 (1995)
17. T. Okuda, A. Asamitsu, Y. Tomioka, T. Kimura, Y. Taguchi, Y. Tokura, Phys. Rev. Lett. **81**, 3203 (1998)
18. B.F. Woodfield, M.L. Wilson, J.M. Byers, Phys Rev. Lett. **78**, 3201 (1997)
19. J.E. Gordon, R.A. Fisher, Y.X. Jia, N.E. Phillips, S.F. Reklis, D.A. Wright, A. Zettl, Phys. Rev. B **59**, 127 (1999)
20. M.R. Lees, O.A. Petrenko, G. Balakrishnan, D. Mck. Paul, Phys. Rev. B **59**, 1298 (1999)
21. L. Ghivelder, I. Abrego Castillo, N.M. Alford, G.H. Tomka, P.C. Riedi, J. MacManus-Driscoll, A.K.M. Akther Hossain, L.F. Cohen, J. Magn. Magn. Mater. **189**, 274 (1998)
22. J.J. Hamilton, E.L. Keatley, H.L. Ju, A.K. Raychaudhuri, V.N. Smolyaninova, R.L. Greene, Phys. Rev. B **54**, 14926 (1996)
23. D. Varshney, K. Choudhary, R.K. Singh, Supercond. Sci. Technol. **15**, 1119 (2002)
24. E.S.R. Gopal, *Specific Heat at Low Temperature* (Plenum, New York, 1966)
25. J.P. Carbotte, Rev. Mod. Phys. **62**, 1027 (1990)
26. C. Kittel, *Quantum Theory of Solids* (John Wiley & Sons, Inc., New York, 1987)
27. R. Mahendiran, S.K. Tiwary, A.K. Raychaudhuri, T.V. Ramakrishanan, R. Mahesh, N. Rangavittal, C.N.R. Rao, Phys. Rev. B **53**, 3348 (1996)
28. J. Blasco, J. Garcia, J.M. de Teresa, M.R. Ibarra, J. Perez, P.A. Algarabel, C. Marquina, C. Ritter, Phys. Rev. B **55**, 8905 (1997)
29. D. Varshney, M.P. Tosi, J. Phys. Chem. Solids **61**, 683 (2000)
30. P. Schiffer, A.P. Ramirez, W. Bao, S.-W. Cheong, Phys. Rev. Lett. **75**, 3336 (1995)
31. W.E. Pickett, D.J. Singh, Phys. Rev. B **53**, 1146 (1996)
32. Y. Tokura, Y. Taguchi, Y. Okada, Y. Fujishima, T. Arima, K. Kumagai, Y. Iye, Phys. Rev. Lett. **70**, 2126 (1993)
33. G.J. Snyder, R. Hiskes, S. DiCarolis, M.R. Beasley, T.H. Geballe, Phys. Rev. B **53**, 14434 (1996)
34. N.W. Ashcroft, N.D. Mermin, *Solid State Physics* (W.B. Saunders Co., New York, 1976), pp. 346
35. P. Fulde, J. Jensen, Phys. Rev. B **27**, 9085 (1983)